# Stark coefficients for highly excited rovibrational states of H2O

M. Grechko, O. Aseev, T. R. Rizzo, N. F. Zobov, L. Lodi, J. Tennyson, O. L. Polyansky, and O. V. Boyarkin

---

## Articles you may be interested in

Ab initio-informed maximum entropy modeling of rovibrational relaxation and state-specific dissociation with application to the O2 + O system
J. Chem. Phys. **144**, 174302 (2016); 10.1063/1.4947590

Highly accurate potential energy surface, dipole moment surface, rovibrational energy levels, and infrared line list for 32S16O2 up to 8000 cm−1
J. Chem. Phys. **140**, 114311 (2014); 10.1063/1.4868327

Rovibrational dynamics of the strontium molecule in the A Σ u + 1 , c3Π u , and a Σ u + 3 manifold from state-of-the-art ab initio calculations
J. Chem. Phys. **136**, 194306 (2012); 10.1063/1.4713939

Communication: Quasiclassical trajectory calculations of correlated product-state distributions for the dissociation of (H2O)2 and (D2O)2
J. Chem. Phys. **135**, 151102 (2011); 10.1063/1.3655564

Dipole moments of HDO in highly excited vibrational states measured by Stark induced photofragment quantum beat spectroscopy
J. Chem. Phys. **122**, 124312 (2005); 10.1063/1.1864912

---

# Stark coefficients for highly excited rovibrational states of $H_2O$

M. Grechko,[1] O. Aseev,[1] T. R. Rizzo,[1] N. F. Zobov,[2] L. Lodi,[3] J. Tennyson,[3,a]
O. L. Polyansky,[2,3] and O. V. Boyarkin[1,a]

[1]*Laboratoire de Chimie Physique Moléculaire (LCPM), École Polytechnique Fédérale de Lausanne,
CH-1015 Lausanne, Switzerland*
[2]*Institute of Applied Physics, Russian Academy of Sciences, Uljanov Street 46,
Nizhnii Novgorod 603950, Russia*
[3]*Department of Physics and Astronomy, University College London, London WC1E 6BT, United Kingdom*

Quantum beat spectroscopy is combined with triple-resonance vibrational overtone excitation to measure the Stark coefficients (SCs) of the water molecule for 28 rovibrational levels lying from 27 600 to 41 000 cm$^{-1}$. These data provide a stringent test for assessing the accuracy of the available potential energy surfaces (PESs) and dipole moment surfaces (DMSs) of this benchmark molecule in this energy region, which is inaccessible by direct absorption. SCs, calculated using the combination of a high accuracy, spectroscopically determined PES and a recent *ab initio* DMS, are within the 1% accuracy of available experimental data for levels below 25 000 cm$^{-1}$, and within 4.5% for coefficients associated with levels up to 35 000 cm$^{-1}$. However, the error in the computed coefficients is over 60% for the very high rovibrational states lying just below the lowest dissociation threshold, due, it seems, to lack of a high accuracy PES in this region. The comparative analysis suggests further steps, which may bring the theoretical predictions closer to the experimental accuracy. © *2012 American Institute of Physics.* [http://dx.doi.org/10.1063/1.4730295]

## I. INTRODUCTION

Energies of rovibrational quantum states of the water molecule and dipole moments of transitions between these levels are the two key components for modeling of absorption and emission spectra of water vapor at any desired temperature. Such spectroscopic information is in high demand for atmospheric photophysics and photochemistry, combustion chemistry, and many other, sometimes exotic, applications. For instance, the presence of free water in such extreme conditions as sunspots[1,2] challenges our ability to predict its spectra at elevated temperatures of about 3500 K. Similar emission from high-lying states of water has been observed in comets, and the mechanism for this phenomenon still remains unexplained.[3] In addition to radiative energy transfer, reactions such as collisional dissociation of water and collisional association of free radicals are of significant interest.[4,5] Reliable simulations of these reactions rely on accurate information on the cross section for collisional energy transfer[6] as well as the molecular energy levels of water. Calculation of these cross sections requires information on the interaction potential between the two colliding particles. One may expect that due to the large permanent and transition dipole moments the leading term in the expansion of the induction energy of the long-range interaction is proportional to the square of the water dipole moment, as in the case for the water-helium complex,[7] for example. Thus, the accuracy of the calculated interaction potential is sensitive to the accuracy of the dipole moment surface (DMS) of the water molecule.

Over many decades 200 000 water-vapor rotational-vibrational transitions have been measured, assigned, and tabulated[8] for use in a variety of different applications. Nevertheless, this still constitutes only a tiny fraction of myriads possible transitions in this small benchmark polyatomic.[9] Complete spectral characterization of the water molecule implies developing a theoretical model, which can be used to calculate any desired transition with spectroscopic accuracy, using a validated potential energy surface (PES), a DMS, and an appropriate computational procedure. Significant advances in computational theory and computer technology means it is now possible to reproduce, *ab initio*, the frequencies of most of the transitions measured within the electronic ground state of water to energy levels below ~25 000 cm$^{-1}$ with a sub-cm$^{-1}$ accuracy[10] and more recently, many transitions close to the dissociation threshold (41 145.94 ± 0.15 cm$^{-1}$) (Refs. 11 and 12) with a less than 10 cm$^{-1}$ discrepancy.[13] Assessing the accuracy with which transition intensities involving high-lying states are reproduced is more difficult for two main reasons. First, the calculation of intensities uses both a potential energy surface and a dipole moment surfaces, and thus accumulates errors from each of them. Second, the experimental accuracy in measuring transition intensities or the associated transition dipole moments is low in this region. Moreover, there are no data at all on the transition dipole moments of water molecule for energy levels above 25 700 cm$^{-1}$. This lack of reference data makes it difficult to verify the accuracy of the available DMS in predicting the intensity of transitions to not only high rovibrational states, but also yet to be measured transitions at lower energies. We address this experimental challenge in this work.

---

[a]Authors to whom correspondence should be addressed. Electronic addresses: oleg.boiarkin@epfl.ch and j.tennyson@ucl.ac.uk.

There are two common experimental techniques to probe the DMS of small polyatomics. First, transition dipole moments can be derived from conventional absorption spectra. However, the use of absorption spectroscopy for the study of $H_2O$ in its electronic ground state is currently limited to the vibrational energies below 25 000 cm$^{-1}$ due to the rapid drop in intensity of overtone transitions with increasing vibrational excitation.[14] The second frequently used approach exploits the Stark effect. The splitting of molecular energy levels in the presence of an external electric field is usually measured using microwave or radio-frequency electromagnetic fields.[15, 16] The data obtained by this method for rotational levels of the vibrational ground and singly excited states of the water have been used to validate and improve the DMS at near equilibrium geometries.[17, 18] However, Doppler broadening, which is typically larger than the Stark splitting, inhibits the extension of such measurements to rotational levels of higher vibrational states. The use of vibrational overtone pre-excitation eliminates problems with Doppler broadening, allowing microwave spectroscopy measurements of Stark splitting in the excited vibrational states to be performed.[19] As an alternative to frequency measurements, Stark splittings can also be measured in the time domain using quantum beat spectroscopy.[20] This technique was employed for measurements of dipole moments of $H_2O$ and HDO in highly vibrationally excited states with $v_{OH} = 4$, 5, and 8 quanta of OH stretch, although only for $J = 1$ rotational levels.[21, 22]

In this work we extend this approach to measure Stark coefficients (SCs) for rovibrational states of water with energies up to the first dissociation limit and in higher rotational states. For the preparation of non-stationary, highly excited rovibrational states we employ triple-resonance vibrational overtone excitation,[13] relying on the spectroscopic data from our recent work.[13, 23–25] The use of the triple-resonance excitation scheme allows access to bound vibrational levels at arbitrary high energy in the electronic ground state of water and facilitates the control of rotational quantum numbers of the excited species. At low vapor pressure, the molecules, once excited, remain collisionally isolated for a few hundreds of ns, during which time we can observe the interference of optical transitions from a coherent superposition of the prepared molecular states by use of a dc electrical field. From the measured frequencies of this interference, called quantum beats, we derive Stark coefficients for the $J = 2$ rotational levels of several vibrational states and for the $J = 3$, $K_a = 0$, $K_c = 3$ level of the $(5,0)^+0$ state. Measured values are compared with Stark coefficients calculated using the latest *ab initio* DMS (Ref. 26) and the latest *ab initio* PES.[13] In addition, Stark coefficients for levels with up to 12 vibrational stretch quanta are calculated using the semi-empirical surface PES$_{12}$ (Ref. 27) in combinations with two different DMS.

## II. EXPERIMENTAL APPROACH

The quantum beat spectroscopy technique is described elsewhere.[20] Here we use it for measurements of splittings of rovibrational levels of $H_2O$ (with rotational quantum numbers $J = 2$ and 3) induced by interaction with an external electric field. The transitions used for preparation of a non-stationary
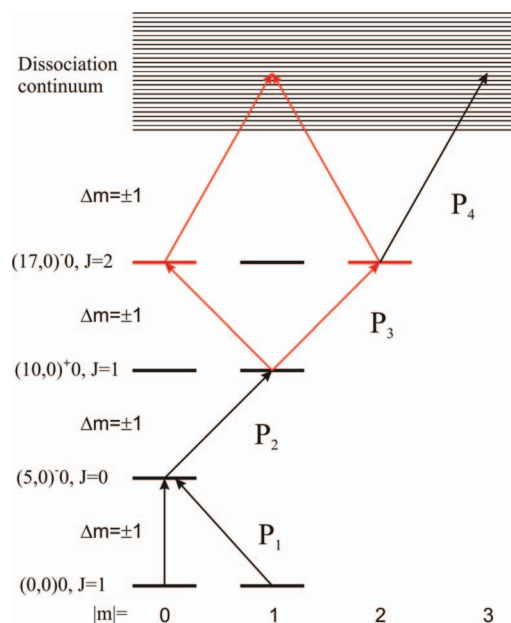


FIG. 1. Schematic energy diagram of excitation pathways employed for coherent excitation (photons $P_1$–$P_3$) of non-stationary states and observation of quantum beats (photon $P_4$). The external electrical field is oriented along the $z$ axis, while linear polarizations of all the lasers are orthogonal to the field. The excitation pathway that leads to quantum beats is shown in red.

state and for probing its evolution, as it is implemented for the $(17, 0)^-0$ vibrational state, are presented in details in Figure 1. Each state is characterized by vibrational quantum numbers in local mode notation $(m, n)^{\pm}v_2$, rotational angular momentum quantum number $J$, and the projection $m$ of this momentum onto $z$ axis, which we define in the direction of the electric field. The linear polarizations of all lasers are orthogonal to the direction of the field.

In this configuration of laser polarizations the selection rules permit electric dipole moment transitions at every excitation step with $\Delta m = \pm 1$ only. In initial thermal equilibrium, the molecules with $J = 1$ equally populate the sublevels with $|m| = 0$, 1. The first laser pulse, $P_1$, promotes a fraction of these molecules to the first intermediate rovibrational level $|(m, n)^{\pm}v_2, J, m\rangle = |(5, 0)^-0, 0, 0\rangle$. The second pulse, $P_2$, promotes molecules from this level to the second intermediate level, which is a superposition of two states with $J = 1$ and $m = +1,-1$: $|\Psi'\rangle \propto |(10, 0)^+0, 1, \pm 1\rangle$. There is no time evolution in this second intermediate level in the presence of the dc electrical field because the sublevels with $m = +1$ and $-1$ remain strictly degenerate. The third laser pulse, $P_3$, coherently prepares the final, non-stationary state

$$|\Psi(0)\rangle = \alpha|(17, 0)^-0, 2, 0\rangle + \beta|(17, 0)^-0, 2, \pm 2\rangle \quad (1)$$

by excitation of a transition from the second intermediate level. Components of this state with $m = 0$ and $m = \pm 2$ in the presence of the field have energies $W_0$ and $W_2$, respectively. The time evolution of the final state is then given by

$$|\Psi(t)\rangle = \alpha|(17, 0)^-0, 2, 0\rangle e^{-\omega_0 t} + \beta|(17, 0)^-0, 2, \pm 2\rangle e^{-\omega_2 t}, \quad (2)$$

where $\omega_r = W_r/\hbar$. After a time delay, $\Delta t$, the fourth laser pulse, $P_4$, promotes the molecules from the final state to the dissociation continuum of the $S_1$ electronic repulsive state. We monitor the number of nascent OH radicals *via* laser-induced fluorescence (LIF). For this we employ the fifth, UV laser pulse, $P_5$ (not shown in Figure 1). The number of dissociated molecules is proportional to the square of the dipole moment of transition from the final state to the dissociation continuum. Because the intensity of the LIF signal is proportional to the number of OH molecules, we can write down the following expression for the signal:

$$S(\Delta t) = S_{const} + S_{osc} \cos[(\omega_2 - \omega_0)\Delta t + \varphi], \quad (3)$$

where the baseline signal $S_{const}$ is modulated by oscillations with amplitude $S_{osc}$, the beat frequency $\omega_2 - \omega_0$ and an initial phase $\phi$.

In order to express the Stark splitting of water levels in an electric field we use perturbation theory. Within second-order perturbation theory the energy of a state $|\Phi_k\rangle$ is given by

$$W_k(E) = W_k^0 + \sum_{l \neq k} \frac{|\langle \Phi_l | \mu_z | \Phi_k \rangle|^2}{W_k^0 - W_l^0} E^2, \quad (4)$$

where $W_k^0$ is the field-free energy of a molecule in state $|\Phi_k\rangle$, $E$ is the strength of the field and the sum runs over all levels of the molecule. The dependence of this energy on quantum number $m$ can be written explicitly

$$W_k(E) = W_k^0 + (A_k + B_k m^2)E^2, \quad (5)$$

where $A_k$ and $B_k$ are the constants, which do not depend on $E$. We thus obtain the following expression for the beat frequency

$$\omega_2 - \omega_0 = 8\pi C_k^{St} E^2, \quad (6)$$

where we have introduced the Stark coefficient $C_k^{St} = B_k/h$. In these terms the measured LIF signal can be expressed as

$$S(\Delta t, E) = S_{const} + S_{osc} \cos\left(8\pi C_k^{St} E^2 \Delta t + \varphi\right). \quad (7)$$

The experimental optical layout we use in this work is similar to that we employed for previous spectroscopic studies of water and is described in details elsewhere.[13,24] For overtone transitions of water with wavenumber higher than $10\,300\ \mathrm{cm}^{-1}$, we use 30–50 mJ output from Nd:YAG pumped dye lasers. For transitions with wavenumber lower than $10\,300\ \mathrm{cm}^{-1}$ we use the first Stokes component generated by stimulated Raman scattering of dye laser beam in hydrogen. To produce the Raman shifted beam, the laser light is focused by a lens with focal length of 30 cm into a cell typically filled with 35 bars of $H_2$. The first Stokes component, whose wavenumber is shifted by $4155.2\ \mathrm{cm}^{-1}$ with respect to the pump dye laser wavenumber and, typically, contains 10 mJ of energy, is separated from the pump beam and other output components by a Pellin-Broca prism. All laser beams are focused and overlapped at the center of the vacuum cell filled with room temperature water vapor at a pressure of $30\ \mu\mathrm{bar}$. We measure the time delay between the third and the fourth laser pulses, $\Delta t$, at each laser shot using a fast photodiode (Thorlabs DET210, 1 ns resolution) and a Hewlett-Packard 54615B digital oscilloscope with 1 GSa/s. We use

two stainless steel electrodes described elsewhere[22] to create a homogeneous electric field. We ground the first electrode and connect the second one to high voltage output of a precision dc power supply (Heinzinger, HNC 20 000), which is personal computer controlled *via* a 12-bit digital-to-analog converter (ACCES I/O PCI-DA12-8). We measure the voltage applied to the electrodes for each data point using a high precision programmable electrometer (Keithley-617) and a voltage divider, calibrated with an accuracy of better than $10^{-5}$. The quantum beat modulations can be recorded as a function of either $\Delta t$ (at a fixed $E$) or $E$ (at fixed $\Delta t$) and we typically scan the field. We fix $\Delta t$ in the range 300 to 1200 ns and minimize time delays between all other laser pulses to about 15 ns.

## III. RESULTS

Figures 2(a) and 2(b) show examples of the LIF signal monitored as function of $E^2$ for two different final rovibrational levels: $(m, n)^{\pm} \nu_2 = (9, 0)^+ 0$, $J_{K_a K_c} = 2_{1,2}$ (Fig. 2(a)) and a final state with energy $W = 40\,984.08\ \mathrm{cm}^{-1}$ (Fig. 2(b), black trace), which is only $161.86\ \mathrm{cm}^{-1}$ below the lowest dissociation threshold of water molecule.[11] Full rovibrational assignment of this high-energy level is ambiguous, and, in addition to the full internal energy, the only strict quantum numbers that we can provide, based on its excitation pathway, are: the total nuclear spin $I = 1$, the angular momentum $J = 2$, and the parity $p = +1$.

In order to derive accurately a beat frequency from the measured LIF signal we, first, eliminate the variation of the baseline by subtraction of a slow varying function of $E^2$ from the experimental trace and Fourier transform the resulting trace (Fig. 2(b), red trace)

$$g(f) = \int_{-\infty}^{+\infty} S_{osc} \cos\left(8\pi C_k^{St} E^2 \Delta t + \varphi\right) e^{-if E^2} dE^2. \quad (8)$$

Figures 2(c) and 2(d) present the Fourier transform $|g(f)|$ of the oscillating term $S_{osc} \cos(8\pi C_k^{St} E^2 \Delta t + \varphi)$ of the signal in Figures 2(a) and 2(b), respectively. The beat frequency is then obtained from a fit of the $|g(f)|$ trace using the function $\mathrm{sinc}(af + b)$. From the fit parameters $a$ and $b$ we calculate quantum beat frequency (in units of $(\mathrm{cm/V})^2$) of the observed signal, $f_0$, using the expression

$$f_0 = -b/a. \quad (9)$$

The Stark coefficient is then given as

$$C_{St} = \frac{f_0}{8\pi \Delta t}. \quad (10)$$

The Stark coefficients, derived from the experimentally observed quantum beats using the procedure described above, are listed in Table I.

## IV. CALCULATIONS OF STARK COEFFICIENTS

When energy $W$, line strength $S(l \leftarrow k)$, Planck constant $h$, and speed of light $c$ are expressed in units of $\mathrm{cm}^{-1}$, (Debye),[2] $J\,s$, and cm/s respectively, the Stark coefficient can
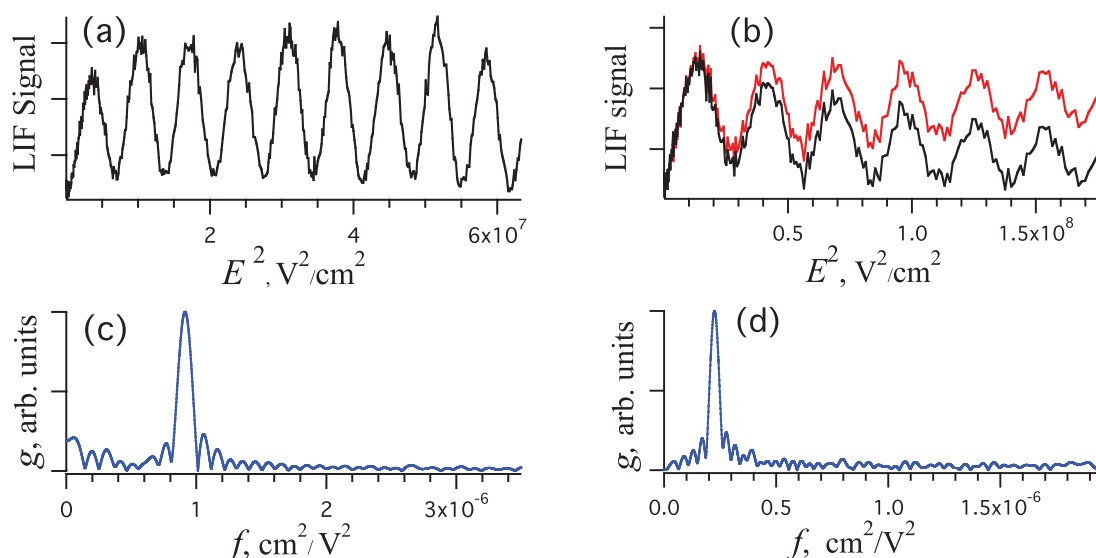
FIG. 2. Observed quantum beat LIF signal as function of square of the applied dc electrical field $E$ for (a) the level $(9,0)^+0$, $2_{1,2}$, (b) the level with total rovibrational energy $E = 40984.08$ cm$^{-1}$, total nuclear spin $I = 1$, rotational quantum number $J = 2$, and parity $p = +1$ (black trace). The levels are prepared via the pathways: (a) $[(9,0)^+0, 2_{1,2}] \leftarrow [(5,0)^+0, 1_{0,1}] \leftarrow [(3,0)^-0, 0_{0,0}] \leftarrow [(0,0)0, 1_{0,1}]$; (b) 40 984.08 cm$^{-1} \leftarrow [(8,0)^+0, 1_{0,1}] \leftarrow [(3,0)^-0, 0_{0,0}] \leftarrow [(0,0)0, 1_{0,1}]$. The red trace (b) is produced from the measured black trace (b) by subtracting its baseline. The Fourier transform functions $|g(f)|$ of the trace (a) and the red trace (b) are shown, respectively, in (c) and (d) (see text for details).

be calculated using the expression[28]

$$C_{St}^k = \frac{k^2}{h^2 c} \sum_{l \neq k} \frac{\begin{pmatrix} J_l & 1 & J_k \\ -1 & 0 & +1 \end{pmatrix}^2 - \begin{pmatrix} J_l & 1 & J_k \\ 0 & 0 & 0 \end{pmatrix}^2}{W_k - W_l},$$

(11)

where $k = 10^{-17}/c$. The measured Stark coefficients provide a stringent test for theoretical models that are designed to calculate molecular spectroscopic data because an accurate calculation of these coefficients requires energy separations, wavefunctions, and transition dipole moments to be determined accurately for all the quantum states involved. This requires a high accuracy potential energy and dipole moment surfaces, as well as a reliable method of performing nuclear motion computations. In practice, for a triatomic system such as water, the rotation-vibration energies and wavefunctions of a given PES can be computed to any desired high accuracy.[10] A comparison of experimental and theoretical values therefore probes the accuracy of the PES and DMS employed. As one can see from Eq. (11), values for the energy levels and line strengths are the ingredients required to compute the Stark coefficients. We use the DVR3D program suite[29] to compute the energy levels and line strengths needed to predict values for the Stark coefficients.

Since the computational cost of a calculation scales rapidly with the size of the used basis set, we employ different basis sets in variational calculations performed for different energy regions of the PES. All calculations were performed in Radau coordinates, with a bisector embedding for states with $J > 0$ to provide convergence better than 0.1 cm$^{-1}$.[30] We note that unlike the case when rotational and vibrational motions are separate,[31] the choice of axis embedding within the

framework of a Hamiltonian that is exact within the Born-Oppenheimer approximation is only a matter of computational efficiency. Energy levels calculated here are converged to better than 0.1 cm$^{-1}$.

Here we employ three different high-accuracy PES, which we designate as SE2011 (a semi-empirical PES),[32] AI2009 (an *ab initio* PES),[13] and PES$_{12}$ (another semi-empirical PES),[27] as well as two different *ab initio* DMS: CVR (Ref. 33) and the recently published LTP2011S surface,[26] to calculate Stark coefficients for rovibrational levels over the entire energy range of the ground electronic state of the water molecule. Calculations with SE2011 PES, which is constructed for energies up to 26 000 cm$^{-1}$, use Morse oscillator-like functions with 29 radial grid points. The angular motions were represented by 40 (associated-)Legendre functions. Final matrices of dimension 1500 were diagonalized to solve the vibrational problem. For rotation-vibration problems, the final matrices had dimensions of $400(J + 1 - p)$, where $J$ is the total angular momentum quantum number and $p$ is the parity. For energy levels up to 34 000 cm$^{-1}$ calculations with the semi-empirical PES$_{12}$ were performed using Morse oscillator-like functions with 50 radial grid points and 40 angular functions. The final vibrational matrix had a dimension of 6000. At higher energies issues with the correct behavior of Morse oscillator-like functions at very short radial separations,[34] associated here with the treatment of linear geometries, mean that alternative basis functions must be used. Calculations up to dissociation with the *ab initio* PES AI2009 used spherical oscillators with 120 grid points and 38 angular functions. In this case the final vibrational matrix was of dimension 15 000.

We use the Eq. (11) and the theoretically calculated values of the energies, wavefunctions, and line strengths to calculate Stark coefficients for rovibrational states of water

TABLE I. Experimental and computed Stark coefficients of $H_2O$.

| State[a] $(m,n)^{\pm} \nu_2, J_{Ka,Kc}$ | Energy, $cm^{-1}$ | $C_{obs}$[b], Hz cm²/V² | $C_1$[c], Hz cm²/V² | $\triangle_1$[d], % | $C_2$[e], Hz cm²/V² | $\triangle_2$[d], % | $C_3$[f], Hz·cm²/V² | $\triangle_3$[d], % | $C_4$[g], Hz·cm²/V² | $\triangle_4$[d], % |
|---|---|---|---|---|---|---|---|---|---|---|
| $(5,0)^{+}0, 3_{0,3}$ | 17024.20 | 0.0222 | … | … | … | … | 0.0230 | 3.6 | … | … |
| $(9,0)^{+}0, 2_{0,2}$ | 27601.26 | 0.00507[g] | 0.0020 | 61* | 0.0017 | 66* | 0.037 | 630* | 0.0365 | 620* |
| $(9,0)^{+}0, 2_{0,2}$ | 27601.26 | 0.00507[g] | 0.0020[h] | 61* | 0.0046 | 9* | … | … | … | … |
| $(9,0)^{+}0, 2_{0,2}$ | 27601.26 | 0.00507[g] | 0.0020[i] | 61* | 0.0047 | 6* | … | … | … | … |
| $(9,0)^{+}0, 2_{0,2}$ | 27601.26 | 0.00507[g] | 0.0020[j] | 61* | 0.0045 | 11* | … | … | … | … |
| $(9,0)^{-}0, 2_{0,2}$ | 27597.40 | 0.05726[k] | 0.0595 | 4 | 0.0584 | 2 | 0.0654 | 14* | 0.0641 | 12* |
| $(9,0)^{+}0, 2_{1,2}$ | 27612.30 | 0.03491[k] | 0.0354 | 1 | 0.0348 | 0.2 | 0.0402 | 15* | 0.0396 | 13* |
| $(9,0)^{-}0, 2_{1,2}$ | 27611.71 | 0.03715[k] | 0.040 | 8 | 0.0395 | 6 | 0.0469 | 26* | 0.0456 | 23* |
| $(9,0)^{+}0, 2_{2,0}$ | 27668.23 | 0.4604[k] | 0.4482 | 3 | 0.4401 | 4 | 0.778 | 69* | 0.7651 | 66* |
| $(9,0)^{-}0, 2_{2,0}$ | 27668.90 | 0.1666[k] | 0.1774 | 7 | 0.1743 | 5 | 0.1704 | 2 | 0.1674 | 1 |
| $(10,0)^{+}0, 2_{0,2}$ | 29867.13 | 0.109[g] | 0.1158 | 6 | 0.1140 | 5 | 0.113 | 4 | 0.1113 | 2 |
| $(10,0)^{-}0, 2_{0,2}$ | 29867.16 | 0.1104[k] | 0.1156 | 5 | 0.1138 | 3 | 0.1155 | 5 | 0.1137 | 3 |
| $(10,0)^{+}0, 2_{1,2}$ | 29873.74 | 0.0465[g] | 0.0487 | 5 | 0.0482 | 4 | 0.0485 | 5 | 0.0481 | 3 |
| $(10,0)^{+}0, 2_{2,0}$ | 29915.13 | 0.471[g] | 0.4760 | 1 | 0.4776 | 1 | 0.487 | 3 | 0.4886 | 4 |
| $(10,0)^{-}0, 2_{2,0}$ | 29915.15 | 0.454[g] | 0.4586 | 1 | 0.4601 | 1 | 0.4734 | 4 | 0.4749 | 5 |
| $(11,0)^{+}0, 2_{0,2}$ | 31964.00 | 0.111[g] | 0.1018 | 8 | 0.1146 | 3 | 0.1173 | 6 | 0.1156 | 4 |
| $(11,0)^{-}0, 2_{0,2}$ | 31963.97 | 0.1113[k] | 0.1174 | 5 | 0.1153 | 4 | 0.1174 | 5 | 0.1156 | 4 |
| $(11,0)^{+}0, 2_{1,2}$ | 31971.01 | 0.04709[k] | 0.0409 | 13 | 0.0485 | 3 | 0.0494 | 5 | 0.0491 | 4 |
| $(11,0)^{-}0, 2_{1,2}$ | 31971.02 | 0.0464[g] | 0.0495 | 7 | 0.0493 | 6 | 0.0481 | 4 | 0.0479 | 3 |
| $(11,0)^{+}0, 2_{2,0}$ | 32011.75 | 0.565[g] | 0.5946 | 5 | 0.6061 | 7 | 0.6046 | 7 | 0.6167 | 9 |
| $(11,0)^{-}0, 2_{2,0}$ | 32011.74 | 0.587[g] | 0.5781 | 2 | 0.5892 | 0.3 | 0.6126 | 4 | 0.6248 | 6 |
| $(12,0)^{+}0, 2_{0,2}$ | 33887.44 | 0.113[g] | 0.120 | 6 | 0.1187 | 5 | 0.1192 | 6 | 0.1178 | 4 |
| $(12,0)^{-}0, 2_{0,2}$ | 33887.46 | 0.1140[k] | 0.1191 | 4 | 0.1178 | 3 | 0.1192 | 5 | 0.1178 | 3 |
| $(12,0)^{+}0, 2_{1,2}$ | 33895.08 | 0.0474[k] | 0.0508 | 7 | 0.0510 | 8 | 0.0494 | 4 | 0.0497 | 5 |
| $(12,0)^{-}0, 2_{1,2}$ | 33895.08 | 0.0468[g] | 0.0495 | 6 | 0.0497 | 6 | 0.0494 | 6 | 0.0497 | 6 |
| $(13,0)^{-}0, 2_{1,2}$ | 35645.90 | 0.0440[g] | … | … | … | | 0.0416 | 6 | 0.0408 | 7 |
| $(14,0)^{+}0, 2_{1,2}$ | 37179.56 | 0.0443[g] | … | … | … | | 0.0443 | 0 | 0.047 | 6 |
| $(14,0)^{-}0, 2_{0,2}$ | 37170.05 | 0.117[l] | … | … | … | | 0.1242 | 6 | 0.1228 | 5 |
| $(15,0)^{-}0, 2_{1,2}$ | 38518.69 | 0.0427[g] | … | … | … | | 0.0220 | 48* | 0.0217 | 49* |
| $(16,0)^{-}0, 2_{0,2}$ | 39618.25 | 0.0846[g] | … | … | … | | 0.1478 | 75* | 0.143 | 69* |
| $(17,0)^{-}0, 2_{0,2}$ | 40494.72 | 0.214[g] | … | … | … | | 0.0698 | 67* | 0.0702 | 67* |
| $J = 2$, ortho, parity = +1 | 40984.08 | 0.0201[g] | … | … | … | | … | … | … | … |
| Average deviation (except the states labeled *),% | | | | 5.2 | | 3.4 | | 4.6 | | 4.4 |

[a]The states are labeled by the three vibrational quantum numbers $(m,n)^{\pm} \nu_2$ in local mode notations and by the asymmetric top rotational quantum numbers $J_{Ka, Kc}$.
[b]Stark coefficients experimentally determined in this work.
[c]Stark coefficients calculated using semi-empirical $PES_{12}$ (Ref. 27) and CVR DMS.[33]
[d]Relative deviation of calculated Stark coefficients from the measured values: $\triangle_i = abs((C_i - C_{obs})/C_{obs}) \cdot 100\%$.
[e]Stark coefficients calculated using semi-empirical $PES_{12}$ (Ref. 27) and LTP2011 DMS.[26]
[f]Stark coefficients calculated using *ab initio* PES2009 (Ref. 13) and CVR DMS.[33]
[g]Stark coefficients calculated using *ab initio* PES2009 (Ref. 13) and LTP2011S DMS (Ref. 26); Accuracy 1%.
[h]Energy of one state with the largest contribution to the Stark coefficient for $(9,0)^{+}0, 2_{0,2}$ level changed to their experimental values.[27]
[i]Energy of two states with the largest contribution to the Stark coefficient for $(9,0)^{+}0, 2_{0,2}$ level changed to their experimental values.[27]
[j]Energy of all three states with the largest contribution to the Stark coefficient for $(9,0)^{+}0, 2_{0,2}$ level changed to their experimental values.[27]
[k]Accuracy 0.5%.
[l]Accuracy 2%.

molecule in the electronic ground state. Tables I and II compare the calculated coefficients with the experimentally determined data.

## V. ANALYSIS

The *ab initio* LTP2011S DMS of water significantly improves the accuracy of calculating intensities of rovibrational transitions in this molecule. In particular, calculations[26] using this DMS reproduce recent line intensities measurements[35] with an accuracy of about 1% which is within the experimental accuracy. It is arguable whether such calculated intensities should replace the measured intensities in standard compilations of water transitions.[36] The measured Stark coefficients presented here and elsewhere[21,22,34] provide an independent opportunity to test the accuracy of this DMS over the whole energy range from the vibrational ground state up to the dissociation threshold.

The earlier calculations of Stark coefficients, which used then the best available PES and DMS surfaces, reproduce the measured coefficients in the 13 800 to 25 000 cm⁻¹ energy interval with an accuracy of only about 3%.[21] The use of

TABLE II. Comparison of the previously measured Stark coefficients of $H_2O$, $C_{obs}$, with calculated in this work.

| State[a] $(m,n)^\pm v_2, J_{Ka,Kc}$ | Energy, $cm^{-1}$ | $C_{obs}$[b], Hz cm$^2$/V$^2$ | $C_1$[c], Hz cm$^2$/V$^2$ | $\triangle_1$[d], % | $C_2$[e], Hz cm$^2$/V$^2$ | $\triangle_2$[d], % |
|---|---|---|---|---|---|---|
| $(0,0)^+0, 1_{11}$ | 37.13 | 0.2267[f] | 0.2298 | 1.4 | 0.2257 | 0.5 |
| $(0,0)^+0, 1_{10}$ | 42.37 | 0.4073[f] | 0.4129 | 1.4 | 0.4055 | 0.4 |
| $(0,0)^+0, 2_{11}$ | 95.17 | 0.0543[f] | 0.0551 | 1.3 | 0.0541 | 0.5 |
| $(0,0)^+1, 1_{11}$ | 1634.96 | 0.1992[f] | 0.2020 | 1.4 | 0.1984 | 0.4 |
| $(0,0)^+1, 1_{10}$ | 1640.50 | 0.3340[f] | 0.3386 | 1.4 | 0.3325 | 0.5 |
| $(0,0)^+1, 2_{11}$ | 1693.64 | 0.0502[f] | 0.0509 | 1.4 | 0.0499 | 0.5 |
| $(1,0)^+0, 1_{10}$ | 3698.49 | 0.4217[f] | 0.4278 | 1.4 | 0.4196 | 0.5 |
| $(1,0)^-0, 1_{11}$ | 3791.70 | 0.2419[f] | 0.2455 | 1.5 | 0.2408 | 0.5 |
| $(1,0)^-0, 1_{10}$ | 3796.98 | 0.4429[f] | 0.4495 | 1.5 | 0.4408 | 0.5 |
| $(4,0)^-0, 1_{01}$ | 13853.27 | 0.4372[g] | 0.4416 | 1 | 0.4318 | 1.2 |
| $(4,0)^-0, 1_{11}$ | 13864.28 | 0.3160[g] | 0.3209 | 1.5 | 0.3115 | 1.4 |
| $(4,0)^-0, 1_{10}$ | 13869.38 | 0.5097[g] | 0.5168 | 1.4 | 0.5047 | 1 |
| $(4,0)^-2, 1_{01}$ | 16844.00 | 0.3153[h] | 0.3224 | 2.3 | 0.3150 | 0.1 |
| $(4,0)^-2, 1_{11}$ | 16859.33 | 0.2137[h] | 0.2137 | 0.0 | 0.2086 | 2.4 |
| $(4,0)^-2, 1_{10}$ | 16865.01 | 0.6306[h] | 0.5936 | 5.9 | 0.6216 | 1.4 |
| $(5,0)^-0, 1_{01}$ | 16920.93 | 0.4277[g] | 0.4345 | 1.6 | 0.4241 | 0.8 |
| $(5,0)^-0, 1_{11}$ | 16932.30 | 0.3032[g] | 0.3074 | 1.4 | 0.2993 | 1.3 |
| $(5,0)^-0, 1_{10}$ | 16937.40 | 0.5077[g] | 0.5180 | 2. | 0.5052 | 0.5 |
| $(8,0)^+0, 1_{01}$ | 25140.60 | 0.4953[g] | 0.5100 | 3.0 | 0.4983 | 0.6 |
| $(8,0)^+0, 1_{11}$ | 25150.12 | 0.4250[g] | 0.4329 | 1.9 | 0.4246 | 0.1 |
| $(8,0)^+0, 1_{10}$ | 25154.61 | 0.6657[g] | 0.6843 | 2.8 | 0.6697 | 0.6 |
| Average deviation | | | | 1.8 | | 0.8 |

[a]The states are labeled by the three vibrational quantum numbers $(m,n)^\pm v_2$ in local mode notations and by the asymmetric top rotational quantum numbers $J_{Ka, Kc}$.
[b]Experimentally determined Stark coefficients.
[c]Stark coefficients calculated using semi-empirical PES$_{12}$ (Ref. 27) and LTP2011S DMS.[26]
[d]Relative deviation of calculated Stark coefficients from the measured values: $\triangle_i = abs((C_i - C_{obs})/C_{obs}) \cdot 100\%$.
[e]Stark coefficients calculated using semi-empirical SE2011 PES (Ref. 32) and LTP2011S DMS (Ref. 26).
[f]Previously measured Stark coefficients taken from Ref. 17.
[g]Previously measured Stark coefficients taken from Ref. 21.
[h]Previously measured Stark coefficients taken from Ref. 22.

the SE2011 PES and LTP2011 DMS results in a significant improvement in the computational accuracy. Tables I and II present the Stark coefficients calculated using three different PESs and two DMSs for three increasingly higher energy ranges. Table II reports the coefficients for the levels lying below 25 000 cm$^{-1}$, calculated with the very accurate SE2011 PES, which is only available for this energy region. Use of wavefunctions and energy differences calculated with this potential dramatically improves our ability to reproduce the measured Stark coefficients. The error in the calculations is reduced from about 3% to below 1%, when the new LTP2011S DMS is used instead of the older ones. These results support the assertion that the LTP2011S DMS is accurate to better than 1% in reproducing intensities of most of the transition to the energy level below 25 000 cm$^{-1}$.

Table I compares the SCs measured here with those calculated using the medium accuracy PES$_{12}$ for computation of energies and wavefunctions of the molecular states with internal energy below 34 000 cm$^{-1}$. We use this PES as it is currently the most accurate in this energy range. Improvements in the results obtained using the LTP2011S DMS are still apparent, although they are less pronounced with an average reduction in the error from 5.2% to 3.4%. The coefficients for the levels in the whole interval covered experimentally,

27 601–40 984 cm$^{-1}$ (except the highest measured level at 40 984.08 cm$^{-1}$), were computed using only a purely *ab initio* PES because there are no semi-empirical surfaces yet available for very highly excited energy levels. The accuracy of the calculations is significantly lower in this case, exhibiting discrepancies with the experimental data of up to 70%, and a huge, above 600%, discrepancy for the levels assigned to the vibrational manifold, originating from the state with nine OH-stretch quanta ($V_{str} = 9$). Apart from these exceptional states, and a few of the highest energy levels, the error in the computed coefficients remains, on average, below 5%. However, there is no significant difference between the results computed with the CVR or the LTP2011S dipole moment surfaces for these high-lying levels, implying that the calculation error in this energy region originates mainly from the PES employed. This conclusion supports the earlier suggestion that the *ab initio* AI2009 PES employed needs significant improvement in the high-energy region.[37,38]

Table I also contains sample results for the $(9, 0)^+0\ 2_{02}$ state, which illustrate how critically the calculated coefficients depend on even small variations in energy for levels involved in near-resonant interactions. The $v_{str} = 9$ vibrational level appears to be split into several sublevels due to anharmonic coupling of, at least, three, near lying resonant vibrational

states.[27] Such mixing makes the predicted Stark coefficients for the vibrational sublevels of the $V_{str} = 9$ manifold particularly sensitive to the calculated energy levels. In a test calculation we replaced, one at a time, the computed energy values of these mixed sublevels by their respective experimental values,[27] each time recalculating SC with the same wavefunctions and DMS. The use of accurate transition frequencies reduces the error in the computed coefficients from 66% down to 6%, demonstrating the importance of having a highly accurate PES for predicting accurate energy spacing.

## VI. CONCLUSIONS

A combination of a triple-resonance vibrational overtone excitation technique and the quantum beat approach is used to detect Stark splittings allowing accurate measurement of Stark coefficients for several highly excited rovibrational levels of the water molecule. Triple-resonance excitation is a proven method for promoting a large fraction of available water molecules to single rovibrational quantum states, lying near (and even above) the dissociation threshold. At the low vapor pressure in our experiments (30 $\mu$bar), laser-excited high-lying states water molecules remain collisionally isolated for up to a few microseconds, giving sufficient time for observation of multiple quantum beats. When combined with careful control and instantaneous measurements of the electrical field and the time delays between laser pulses, Stark coefficients can be determined with an experimental accuracy of better than 1%. The technique is used for 28 rovibrational levels lying between 27 600 and 40 980 cm$^{-1}$. These data are used to evaluate the accuracy of the available potential and dipole moment surfaces of water.

The accuracy of the calculated SCs presented here clearly differs in three energy regions. The use of a new, highly accurate *ab initio* DMS for calculating SC greatly improves the theoretical results but these depend strongly on the quality of the corresponding PES. At lower energies, where a PES is available which reproduces the observed energy levels to within 0.02 cm$^{-1}$, use of the LTP2011S DMS gives a dramatic improvement: our results give a 4-fold improvement in accuracy of the SC calculations compared to the best previously published results. In this region the accuracy of the calculated SC is comparable to the corresponding experimental accuracy—better than 1%. For levels up to 35 000 cm$^{-1}$, where a reasonably accurate (energy levels to within about 0.3 cm$^{-1}$), semi-empirical PES is available, SC are calculated with an accuracy of about 4%. In this region, the use of a better DMS results only in a 30% improvement in accuracy as the quality of the new DMS is camouflaged by the relative inaccuracy of the PES used. For high-lying energy levels, where there is no available semi-empirically fitted PES and the best *ab initio* PES only reproduces the observed energy levels with an accuracy of about 10 cm$^{-1}$, the computed Stark coefficients generally differ from the observed ones by more than 50%. Here the error in the Stark coefficient calculation is completely determined by the relative inaccuracy of the PES; these calculations are insensitive to the choice of DMS.

Our overall conclusion is that spectroscopic procedure presented here provides an excellent, independent tool for calibrating the quality of a PES and a DMS. At present our Stark coefficient calculations are very accurate with the newly constructed *ab initio* DMS when a correspondingly accurate PES is available. However, when a spectroscopic quality PES is not available, it is only by further improvement of the PES, or the use of empirical energy levels, that it is possible to calculate SCs with an accuracy close to the experimental one.

[1] L. Wallace, P. Bernath, W. Livingston, K. Hinkle, J. Busler, B. J. Guo, and K. Q. Zhang, Science **268**, 1155 (1995).

[2] O. L. Polyansky, N. F. Zobov, S. Viti, J. Tennyson, P. F. Bernath, and L. Wallace, Science **277**, 346 (1997).

[3] R. J. Barber, S. Miller, N. Dello Russo, M. J. Mumma, J. Tennyson, and P. Guio, MNRAS **398**, 1593 (2009).

[4] R. Atkinson, D. L. Baulch, R. A. Cox, J. N. Crowley, R. F. Hampson, R. G. Hynes, M. E. Jenkin, M. J. Rossi, and J. Troe, Atmos. Chem. Phys. **4**, 1461 (2004).

[5] D. L. Baulch, C. T. Bowman, C. J. Cobos, R. A. Cox, T. Just, J. A. Kerr, M. J. Pilling, D. Stocker, J. Troe, W. Tsang, R. W. Walker, and J. Warnatz, J. Phys. Chem. Ref. Data **34**, 757 (2005).

[6] J. Troe, Annu. Rev. Phys. Chem. **29**, 223 (1978).

[7] M. P. Hodges, R. J. Wheatley, and A. H. Harvey, J. Chem. Phys. **116**, 1397 (2002).

[8] J. Tennyson *et al.*, "IUPAC critical evaluation of the rotational-vibrational spectra of water vapor. Part III. Energy levels and transition wavenumbers for H$_2$ $^{16}$O," J. Quant. Spectrosc. Radiat. Transf. (submitted).

[9] R. J. Barber, J. Tennyson, G. J. Harris, and R. N. Tolchenov, MNRAS **368**, 1087 (2006).

[10] O. L. Polyansky, A. G. Csaszar, S. V. Shirin, N. F. Zobov, P. Barletta, J. Tennyson, D. W. Schwenke, and P. J. Knowles, Science **299**, 539 (2003).

[11] P. Maksyutenko, T. R. Rizzo, and O. V. Boyarkin, J. Chem. Phys. **125**, 181101 (2006).

[12] O. L. Polyansky, N. F. Zobov, I. I. Mizus, L. Lodi, S. N. Yurchenko, J. Tennyson, A. G. Csaszar, and O. V. Boyarkin, Philos. Trans. R. Soc. A **370**, 2728 (2012).

[13] M. Grechko, O. V. Boyarkin, T. R. Rizzo, P. Maksyutenko, N. F. Zobov, S. V. Shirin, L. Lodi, J. Tennyson, A. G. Csaszar, and O. L. Polyansky, J. Chem. Phys. **131**, 221105 (2009).

[14] P. Dupre, T. Gherman, N. F. Zobov, R. N. Tolchenov, and J. Tennyson, J. Chem. Phys. **123**, 154307 (2005).

[15] S. A. Clough, Y. Beers, G. P. Klein, and L. S. Rothman, J. Chem. Phys. **59**, 2254 (1973).

[16] T. R. Dyke and J. S. Muenter, J. Chem. Phys. **59**, 3125 (1973).

[17] S. L. Shostak and J. S. Muenter, J. Chem. Phys. **94**, 5883 (1991).

[18] M. Mengel and P. Jensen, J. Mol. Spectrosc. **169**, 73 (1995).

[19] J. S. Muenter, J. Rebstein, A. Callegari, and T. R. Rizzo, J. Chem. Phys. **111**, 3488 (1999).

[20] E. Hack and J. R. Huber, Int. Rev. Phys. Chem. **10**, 287 (1991).

[21] A. Callegari, P. Theule, J. S. Muenter, R. N. Tolchenov, N. F. Zobov, O. L. Polyansky, J. Tennyson, and T. R. Rizzo, Science **297**, 993 (2002).

[22] P. Theule, A. Callegari, T. R. Rizzo, and J. S. Muenter, J. Chem. Phys. **122**, 124312 (2005).

[23] M. Grechko, P. Maksyutenko, N. F. Zobov, S. V. Shirin, O. L. Polyansky, T. R. Rizzo, and O. V. Boyarkin, J. Phys. Chem. A **112**, 10539 (2008).

[24] M. Grechko, P. Maksyutenko, T. R. Rizzo, and O. V. Boyarkin, J. Chem. Phys. **133**, 81103 (2010).

[25] P. Maksyutenko, M. Grechko, T. R. Rizzo, and O. V. Boyarkin, Philos. Trans. R. Soc. A **370**, 2710 (2012).

[26] L. Lodi, J. Tennyson, and O. L. Polyansky, J. Chem. Phys. **135**, 034113 (2011).

[27]P. Maksyutenko, J. S. Muenter, N. F. Zobov, S. V. Shirin, O. L. Polyansky, T. R. Rizzo, and O. V. Boyarkin, J. Chem. Phys. **126**, 241101 (2007).

[28]See supplementary material at http://dx.doi.org/10.1063/1.4730295 for details on derivation of Eq. (11).

[29]J. Tennyson, M. A. Kostin, P. Barletta, G. J. Harris, O. L. Polyansky, J. Ramanlal, and N. F. Zobov, Comput. Phys. Commun. **163**, 85 (2004).

[30]J. Tennyson and B. T. Sutcliffe, Int. J. Quantum Chem. **42**, 941 (1992).

[31]C. R. Le Sueur, S. Miller, J. Tennyson, and B. T. Sutcliffe, Mol. Phys. **76**, 1147 (1992).

[32]I. I. Bubukina, N. F. Zobov, O. L. Polyansky, S. V. Shirin, and S. N. Yurchenko, Opt. Spectrosc. **110**, 160 (2011).

[33]L. Lodi, R. N. Tolchenov, J. Tennyson, A. E. Lynas-Gray, S. V. Shirin, N. F. Zobov, O. L. Polyansky, A. G. Csaszar, J. N. P. van Stralen, and L. Visscher, J. Chem. Phys. **128**, 44304 (2008).

[34]J. Tennyson and B. T. Sutcliffe, J. Mol. Spectrosc. **101**, 71 (1983).

[35]D. Lisak, D. K. Havey, and J. T. Hodges, Phys. Rev. A **79**, 52507 (2009).

[36]L. Lodi and J. Tennyson, J. Quant. Spectrosc. Radiat. Transf. **113**, 850 (2012).

[37]A. G. Csaszar, E. Matyus, T. Szidarovszky, L. Lodi, N. F. Zobov, S. V. Shirin, O. L. Polyansky, and J. Tennyson, J. Quant. Spectrosc. Radiat. Transf. **111**, 1043 (2010).

[38]N. F. Zobov, S. V. Shirin, L. Lodi, B. C. Silva, J. Tennyson, A. G. Csaszar, and O. L. Polyansky, Chem. Phys. Lett. **507**, 48 (2011).